Co-published by
Institute of Fluid-Flow Machinery
Polish Academy of Sciences
Committee on Thermodynamics and Combustion
Polish Academy of Sciences

Copyright©2026 by the Authors under licence CC BY-NC-ND 4.0

http://www.imp.gda.pl/archives-of-thermodynamics/

Numerical investigation of a double twisted tube heat exchanger in different configurations

Ali K. Abdul Razzaq[a*], Khudheyer S. Mushatet[b], Riyam Ali Khaled[c]

[a]Iraq Ministry of Defense, Al-Nasiriyah 64001, Iraq
[b]University of Thi-Qar, Al-Nasiriyah 64001, Iraq
[c]Ministry of Oil, Thi-Qar Oil Company, Al-Nasiriyah 64001, Iraq
[*]Corresponding author email: aliengn717@gmail.com

Received: 05.09.2025; revised: 09.02.2026; accepted: 25.02.2026

Abstract

This study investigates the thermal and hydraulic performance of three configurations of double twisted tube heat exchangers (DTTHEs): circular (DCTTHE), elliptical (DETTHE) and square (DSTTHE) tubes, all with a twist ratio of 5. Numerical simulations were performed using Ansys Fluent with the *k*-*ε* turbulence model at Reynolds numbers ranging from 5000 to 25 000 to analyse heat transfer enhancement mechanisms. The working fluids were hot water and cold water, with varied inlet mass flow rates. Key performance parameters, such as the Nusselt number, overall heat transfer coefficient, pressure drop and effectiveness, were computed. Results demonstrate that DETTHE outperforms the other configurations, achieving superior heat transfer efficiency due to intensified secondary flows and vortices that enhance fluid mixing and disrupt thermal boundary layers. DETTHE exhibited the highest overall heat transfer coefficient, Nusselt number and effectiveness, with a maximum improvement in overall performance factor of approximately 74% and 300%, compared to DCTTHE and DSTTHE, respectively. However, this enhancement came at the cost of higher pressure drops. Temperature contours revealed uniform thermal distribution and improved heat exchange in DETTHE, particularly at the outlet region. Enhanced turbulence, secondary flow generation and stronger mixing near the tube walls contributed to these improvements. The study highlights the trade-off between thermal performance and hydraulic losses. The findings from this comparative analysis provide insights into the relative performance of different double twisted tube designs. Among the designs, DETTHE achieved the highest performance factor, making it a promising solution for compact and high-efficiency industrial heat exchangers.

Keywords: Twisted tube heat exchanger; Thermal-hydraulic performance; Double-tube heat exchanger; Heat transfer enhancement

Vol. 47(2026), No. 3, 139–146; doi: 10.24425/ather.2026.7512

Cite this manuscript as Razzaq, A.K.A., Mushatet, K.S., & Khaled, R.A. (2026). Numerical investigation of a different configurations double twisted tube heat exchanger. *Archives of Thermodynamics*, 47(3), 139–146.

1. Introduction

Heat exchangers play a vital role in numerous industrial and engineering applications, making their design a multifaceted and demanding discipline. Beyond financial and durability considerations, thorough hydraulic and thermal performance analysis is essential in their development [1]. Strategies to enhance thermal efficiency frequently involve a trade-off; for instance, design features that intensify heat transfer (e.g. fins, baffles, twist tape, twist tube or surface roughening) often simultaneously increase hydraulic resistance, leading to higher pressure drops and greater pumping power requirements.

Heat transfer enhancement techniques fall into two categories: active and passive. Among these, passive methods have attracted significant attention due to their cost efficiency and simplicity [2]. A common passive approach involves flow-modifying devices like twisted tape, which generates secondary flows alongside axial motion, intensifying turbulence. This enhanced

Nomenclature

A_s – heat transfer surface area, m^2
C – heat capacity rate, W/K
C_p – specific heat, J/(kg K)
d – inner tube diameter, m
D – outer tube diameter, m
D_h – hydraulic diameter, m
k – turbulent kinetic energy, J/kg
L – length, m
LMTD – logarithmic mean temperature difference, K
$\dot{m}$ – mass flow rate, kg/s
p – twist pitch, mm
P – pressure, Pa
ΔP_T – total pressure drop, Pa
Q_{avg} – average heat transfer rate, W
Re – Reynolds number, Re $= Du\rho/\mu$
t – time, s
T – temperature, K
Tr – twisted ratio
u, v, w – velocity components, m/s
U – overall heat transfer coefficient, W/(m^2 K)
x, y, z – Cartesian coordinates, m

Greek symbols

Γ – thermal conductivity, W/(m^2 K)
ε – turbulent energy dissipation, m^2/s^3
ϵ – heat exchanger effectiveness
η – overall performance index, 1/Pa
μ – dynamic viscosity, Pa s
ρ – density, kg/m^3

Subscripts and Superscripts

c – cold
eff – effective
h – hot
i – inlet
o – outlet
t – turbulent

Abbreviations and Acronyms

DCTTHE – double circular twisted tube heat exchanger
DETTHE – double elliptical twisted tube heat exchanger
DSTTHE – double square twisted tube heat exchanger

mixing reduces the boundary layer thickness within the heat exchanger tube [3].

A critical synthesis of the literature on heat transfer enhancement using twisted geometries reveals a complex landscape defined by significant advancements, yet marked by persistent methodological gaps and unresolved questions regarding optimal configuration and scalability. The existing body of work can be broadly categorised and critically evaluated along several thematic lines. A primary focus has been on the geometric evolution from simple inserts to complex channel shapes. Early investigations effectively established the foundational principle that swirl flow induces thinning of the thermal boundary layer and improves fluid mixing. Studies employing twisted tape inserts, such as those by Salam et al. [3] and Murali et al. [4], consistently demonstrate this, reporting Nusselt number enhancements of 2.3−2.9 times and 1.4−1.8 times higher friction factors compared to smooth tubes. However, a critical limitation of this approach is the inherent trade-off between heat transfer augmentation and pressure drop, as the solid tape core significantly obstructs flow. This limitation prompted a shift towards twisted tubes themselves (e.g. elliptical, oval), which generate swirl without a central obstruction. For instance, Wu et al. [5] and Cheng et al. [6] found that twisted elliptical and oval tubes improve the synergy between the velocity vector and the temperature gradient, achieving performance evaluation criteria (PEC) in the range of 1.6−1.7. This transition from inserts to integral twisted geometries represents a pivotal development, moving towards systems that enhance heat transfer more efficiently by working with the flow path rather than obstructing it.

Within the domain of twisted tubes, a critical analytical gap emerges concerning the comparative impact of different geometric parameters under consistent flow regimes. For instance, while Cheng et al. [6] and Luo et al. [7] both investigated twisted oval tubes, their studies were confined to laminar flow (Reynolds numbers less than 2000). Their findings on the optimal twist pitch are not directly transferable to the turbulent regime studied by Alempour et al. [8] (Reynolds numbers ranging from 4000 to 16 000). This creates a significant knowledge gap: the interaction between twist pitch, aspect ratio and flow regime is poorly understood, making it difficult to predict performance across different operational scales. Furthermore, the work of Kim et al. [9] added another layer of complexity, suggesting that for twisted elliptic tubes, the number of revolutions has a substantial impact on thermal performance, while the aspect ratio's variation is "negligible" – a conclusion that may be specific to their chosen geometric range and contradicts the importance placed on flattening ratios in other studies like Cheng et al. [6]. This apparent contradiction underscores the lack of a unified geometric optimisation framework.

The pursuit of further enhancement has led to hybrid systems, which combine twisted geometries with nanofluids. The research of Mushatet and Youssif [10,11], Alempour et al. [8], and others consistently show a synergistic effect. For example, Mushatet and Youssif [11] reported a remarkable 214% heat transfer enhancement using Al_2O_3/water nanofluid in a tube with a twin twisted tape insert. However, a critical analysis of these hybrid studies reveals a common, and potentially limiting, methodological trend: a heavy reliance on numerical simulations [8,10–12] or highly controlled experimental setups. While these approaches are invaluable for parametric analysis, they often fail to fully capture the long-term practical challenges, such as nanoparticle sedimentation, corrosion, and increased pumping power costs associated with the compounded pressure drops from both the twist and the nanofluid, as noted by Karimi et al. [13].

This synthesis exposes a critical and underexplored niche in the literature. First, there is a pronounced disconnect between studies focused on geometric optimisation and those investigating hybrid nanofluid applications; few works systematically dissect whether the performance gains from a hybrid system are

due to a truly optimal geometry or simply the additive effect of the nanofluid. Second, the literature is heavily fragmented according to flow regimes, with most studies operating exclusively in either laminar [5,7,8] or turbulent [4,11,12] conditions, with a notable scarcity of research that bridges this divide. Finally, there is an overreliance on numerical models that have not been extensively validated against experimental data for the specific combination of complex geometries and nanofluids.

This study explores the thermal performance of double-twisted-tube heat exchangers by analysing three geometric configurations: circular, elliptical and square. Using 3D computational modelling, the research assesses the flow behaviour, heat transfer efficiency and overall system effectiveness across different twisted tube designs. A mesh independence analysis was performed, with stringent checks on mesh quality (including orthogonal quality and aspect ratio) to ensure solution accuracy in Ansys Fluent. Furthermore, critical dimensionless parameters – such as Reynolds number, Nusselt number and overall performance metrics – were computed, alongside a detailed evaluation of average heat transfer rates and exchanger effectiveness.

2. Mathematical analysis

The study examines three configurations of twisted double-tube heat exchangers, each with a twist ratio (Tr = p/D, where p denotes the twist pitch and D denotes the outer tube diameter) of 5 and a uniform tube thickness of 4 mm. The first design illustrated in Fig. 1 (left side) features circular tubes, with an inner tube diameter (d_i) of 18 mm and an outer tube diameter (D_i) of 50 mm, spanning a length (L) of 1 m. In this counter-flow arrangement, hot water passes through the inner tube while cold water flows through the outer annular space, with varying mass flow rates tested for both fluids. The second configuration, illustrated in Fig. 1 (middle), employs elliptical twisted tubes with semi-major and semi-minor radii of 13 mm and 6.3 mm, respectively. The third design, depicted in Fig. 1 (right side), utilises square twisted tubes with side lengths of 15.9 mm (inner) and 44.3 mm (outer). All models are constructed from aluminium and share identical operational parameters for comparative analysis.

The dynamics of fluid flow are governed by fundamental conservation laws — mass, momentum, and energy —which form the basis for numerical simulations and analytical solutions in fluid mechanics. The continuity equation enforces the principle of mass conservation, ensuring that the combined mass flow rate at the inlets is equal to that at the outlets:

$$\frac{\partial(\rho u)}{\partial x}+\frac{\partial(\rho v)}{\partial y}+\frac{\partial(\rho w)}{\partial z}=0, \tag{1}$$

where u, v, and w are the velocity vector components, ρ is the density, and x, y and z are the Cartesian coordinates. Alongside the momentum and energy equations, this framework enables precise modelling and analysis of fluid behaviour under varying conditions [14].

Within this investigation, the Navier-Stokes equations govern momentum conservation, enabling precise evaluation of pressure and velocity profiles across the heat exchanger [15]:

$$\left(\frac{\partial u^2}{\partial x}+\frac{\partial uv}{\partial y}+\frac{\partial uw}{\partial z}\right)=-\frac{1}{\rho}\frac{\partial P}{\partial x}+\frac{\partial}{\partial x}\left(2\mu_{eff}\frac{\partial u}{\partial x}\right)+\frac{\partial}{\partial y}\left(\mu_{eff}\frac{\partial u}{\partial y}\right)+$$
$$+\frac{\partial}{\partial z}\left(\mu_{eff}\frac{\partial u}{\partial z}\right)+\frac{\partial}{\partial y}\left(\mu_{eff}\frac{\partial v}{\partial x}\right)+\frac{\partial}{\partial z}\left(\mu_{eff}\frac{\partial w}{\partial x}\right), \tag{2}$$

$$\left(\frac{\partial vu}{\partial x}+\frac{\partial v^2}{\partial y}+\frac{\partial vw}{\partial z}\right)=-\frac{1}{\rho}\frac{\partial P}{\partial x}+\frac{\partial}{\partial x}\left(\mu_{eff}\frac{\partial v}{\partial x}\right)+\frac{\partial}{\partial y}\left(2\mu_{eff}\frac{\partial v}{\partial y}\right)+$$
$$+\frac{\partial}{\partial z}\left(\mu_{eff}\frac{\partial v}{\partial z}\right)+\frac{\partial}{\partial x}\left(\mu_{eff}\frac{\partial u}{\partial y}\right)+\frac{\partial}{\partial z}\left(\mu_{eff}\frac{\partial w}{\partial y}\right), \tag{3}$$

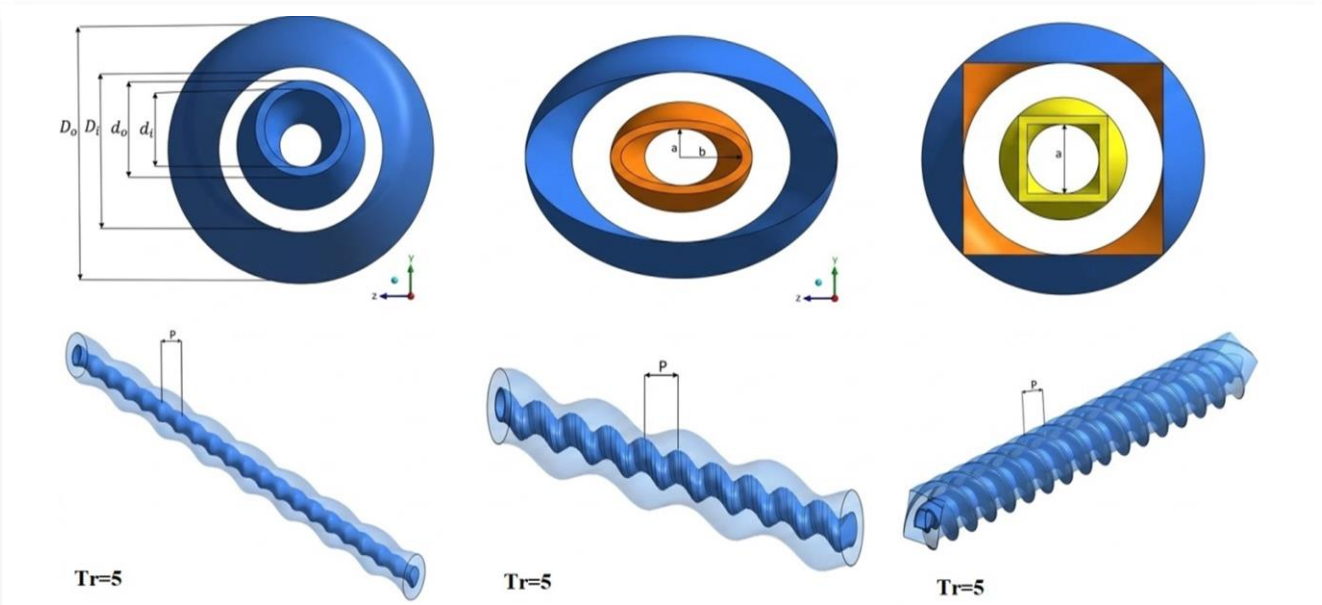


Fig. 1. A schematic illustration of a dual-loop heat exchanger configurations (circular tube, elliptical tube, square tube); cross-sections and 3D isometric views.

$$\left(\frac{\partial wu}{\partial x}+\frac{\partial wv}{\partial y}+\frac{\partial w^2}{\partial z}\right)=-\frac{1}{\rho}\frac{\partial P}{\partial x}+\frac{\partial}{\partial x}\left(\mu_{eff}\frac{\partial w}{\partial x}\right)+\frac{\partial}{\partial y}\left(\mu_{eff}\frac{\partial w}{\partial y}\right)+$$
$$+\frac{\partial}{\partial z}\left(2\mu_{eff}\frac{\partial w}{\partial z}\right)+\frac{\partial}{\partial x}\left(\mu_{eff}\frac{\partial u}{\partial z}\right)+\frac{\partial}{\partial y}\left(\mu_{eff}\frac{\partial v}{\partial z}\right). \quad (4)$$

where P is the pressure and μ_{eff} is the effective dynamic viscosity.

The energy conservation equation governs thermal energy transfer within fluid systems by accounting for heat exchange and mechanical work. In this analysis, it enables precise determination of temperature fields and heat flux across the heat exchanger's fluid and solid domains. The governing energy equation for fluid flow is expressed as [15]:

$$\frac{\partial uT}{\partial x}+\frac{\partial vT}{\partial y}+\frac{\partial wT}{\partial z}=\frac{\partial}{\partial x}\left(\Gamma_{eff}\frac{\partial T}{\partial x}\right)+\frac{\partial}{\partial y}\left(\Gamma_{eff}\frac{\partial T}{\partial y}\right)+$$
$$+\frac{\partial}{\partial z}\left(\Gamma_{eff}\frac{\partial T}{\partial z}\right), \quad (5)$$

where T is the temperature and Γ_{eff} represents the overall (effective) thermal conductivity.

In the above equations, effective parameters are described as follows [15]:

$$\mu_{eff}=\mu+\mu_t, \quad (6)$$

$$\Gamma_{eff}=\Gamma+\Gamma_t, \quad (7)$$

where μ and μ_t represent the viscosity as the baseline physical property and the turbulent dynamic viscosity, respectively. The latter becomes zero for laminar flow. Similarly, Γ and Γ_t denote the intrinsic/baseline and turbulent thermal conductivity, respectively.

The current investigation employs the k-ε turbulence model for analysing the outer boundary layer region. Selected for its computational efficiency and predictive reliability, this model demonstrates exceptional capability in resolving turbulent flow characteristics adjacent to solid boundaries while ensuring numerical stability in undisturbed flow regions. Particularly advantageous for complex flow geometries, the model accurately predicts separation phenomena and manages adverse pressure gradients. It was applied to account for the turbulent boundary-layer interactions that are central to the present study, as expressed by the governing equations below [15]:

$$\rho\left(\frac{\partial}{\partial x}(ku)+\frac{\partial}{\partial y}(kv)+\frac{\partial}{\partial z}(kw)\right)=\frac{\partial}{\partial x}\left(\frac{\mu_t}{\sigma_k}\frac{\partial k}{\partial x}\right)+\frac{\partial}{\partial y}\left(\frac{\mu_t}{\sigma_k}\frac{\partial k}{\partial y}\right)$$
$$+\frac{\partial}{\partial z}\left(\frac{\mu_t}{\sigma_k}\frac{\partial k}{\partial z}\right)+G-\rho\varepsilon, \quad (8)$$

$$\rho\left(\frac{\partial}{\partial x}(\varepsilon u)+\frac{\partial}{\partial y}(\varepsilon v)+\frac{\partial}{\partial z}(\varepsilon w)\right)=\frac{\partial}{\partial x}\left(\frac{\mu_t}{\sigma_\varepsilon}\frac{\partial \varepsilon}{\partial x}\right)+\frac{\partial}{\partial y}\left(\frac{\mu_t}{\sigma_\varepsilon}\frac{\partial \varepsilon}{\partial y}\right)$$
$$+\frac{\partial}{\partial z}\left(\frac{\mu_t}{\sigma_\varepsilon}\frac{\partial \varepsilon}{\partial z}\right)+C_{1\varepsilon}\rho\frac{\varepsilon}{k}G-C_{2\varepsilon}\rho\frac{\varepsilon^2}{k}, \quad (9)$$

where k is the turbulent kinetic energy, G represents the rate of its production per unit volume, ε is the turbulence dissipation rate, and $C_{1\varepsilon}$ = 1.44, $C_{2\varepsilon}$ = 1.92, σ_k = 1, σ_ε = 1.3.

The twisted tube configuration introduces a paradigm in double-tube heat exchanger design, demanding comprehensive characterisation of key thermal-hydraulic parameters. Critical numbers including Reynolds and Nusselt, along with friction factor, effectiveness and heat transfer coefficients, form the fundamental framework for performance prediction and optimisation. This investigation employs the following relations [16]:

$$\mathrm{Re}=\frac{\rho D_h u}{\mu}, \quad (10)$$

$$D_{h,i}=d_i, \quad (11)$$

$$D_{h,o}=D_i-d_o, \quad (12)$$

where $D_{h,i}$ and $D_{h,o}$ denote the hydraulic diameter of the inner and outer tube, respectively.

The logarithmic mean temperature difference is expressed by [16]

$$\mathrm{LMTD}=\frac{\Delta T_1-\Delta T_2}{\ln\left(\frac{\Delta T_1}{\Delta T_2}\right)}, \quad (13)$$

where

$$\Delta T_1=T_{hi}-T_{co}, \quad (14)$$

$$\Delta T_2=T_{ho}-T_{ci}. \quad (15)$$

In the above, subscripts h and c refer to hot and cold fluid, respectively, whereas subscripts i and o stand for inlet and outlet, respectively.

The effectiveness of a heat exchanger is defined as [16]

$$\epsilon=\frac{q_{act}}{q_{max}}, \quad (16)$$

where

$$q_{act}=C_c(T_{co}-T_{ci}), \quad (17)$$

$$q_{max}=C_{min}(T_{hi}-T_{ci}), \quad (18)$$

where C_{min} is the lower value of capacity rates C_h or C_c:

$$C_h=\dot{m}_h C_{ph}, \qquad C_c=\dot{m}_c C_{pc},$$

where C_p is the specific heat and $\dot{m}$ is the mass flow rate.

The Nusselt number and convective heat transfer coefficient are given as, respectively:

$$\mathrm{Nu}=\frac{h D_h}{K_f}, \quad (19)$$

$$h=\frac{\dot{m}_h C_{ph}(T_i-T_o)}{A_s(T_m-T_s)}, \quad (20)$$

where A_s is the heat transfer surface area, K_f is the thermal conductivity of the fluid, T_s is the wall temperature and T_m is bulk temperature of the fluid.

The overall performance index can be expressed as follows [17]:

$$\eta=\frac{\epsilon}{\Delta P_T}, \quad (21)$$

where ΔP_T is the total pressure drop.

3. Mesh modelling and mesh independence

The computational domain was created using Ansys Design Modeler (2023R1) and meshed within the Ansys Workbench environment. To accurately resolve the critical flow physics, a hybrid meshing strategy was employed. This involved the use of

Table 1. Meshing independence.

DETTHE			DCTTHE			DSTTHE		
No. of grid elements	*U*	*U*, deviation	No. of grid elements	*U*	*U*, deviation	No. of grid elements	*U*	*U*, deviation
1789045	1650	0.09	468384	569.19	0.0300	2321543	1350	0.07
2120000	1810	0.03	761362	585.12	0.0087	2865097	1450	0.03
2527348*	1879	0.01	1208000*	590.22	0.0055	3155185*	1495	0.02
2956732	1910	–	1782044	593.45	–	3754321	1533	–

*) mesh size selected for further analysis

tetrahedral elements in the core volume, coupled with disciplined inflation layers at the walls to capture near-wall gradients, and targeted local refinement in regions prone to high velocity gradients and flow separation, such as the lee of the helical twists.

A mesh independence study was conducted, monitoring key performance parameters (e.g. Nusselt number and pressure drop). As detailed in Table 1, the solution demonstrated stability for the selected mesh (marked with an asterisk), with variations in the overall heat transfer coefficient below a predefined threshold of, e.g., 1% upon further refinement. This confirms that the computational results are quantitatively independent of the mesh discretisation, providing confidence in the reliability of the subsequent simulation data.

4. Boundary conditions

The numerical simulations commenced upon implementing the prescribed boundary conditions. For the hot water stream, multiple mass flow rates were examined to investigate varying thermal-hydraulic conditions, while maintaining a constant flow rate for the cold water circuit. The study explored Reynolds numbers ranging from 5000 to 25 000, with fixed inlet temperatures of 25°C for the cold fluid and 70°C for the hot fluid. Adiabatic conditions were imposed on all external surfaces to ensure thermal isolation of the system.

5. Results and discussion

Figure 2 illustrates the variation in hot fluid outlet temperature for the DCTTHE, DETTHE and DSTTHE configurations as a function of Reynolds number at Tr = 5. The DETTHE configuration exhibits the lowest outlet temperature due to enhanced heat transfer from the cold fluid. In contrast, the DCTTHE shows a consistently higher outlet temperature compared to both DSTTHE and DETTHE across all Reynolds numbers, primarily because it generates less turbulence than the other configurations.

Figure 3 illustrates the variation of the cold fluid outlet temperature (T_{co}) with Reynolds number for the DCTTHE, DSTTHE and DETTHE configurations at a twist ratio (Tr = 5). DETTHE presents the highest outlet temperatures across all Reynolds values, followed by DSTTHE, while DCTTHE exhibits the lowest T_{co}. This behaviour can be attributed to the more pronounced swirl motion and stronger secondary vortices generated within DETTHE, which enhance mixing and intensify local convective heat transfer. In contrast, although DCTTHE

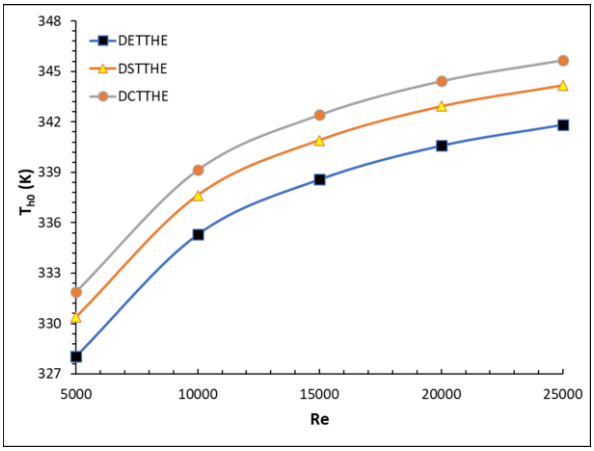


Fig. 2. Variation of the hot water outlet temperature with Reynolds number for DCTTHE, DSTTHE and DETTHE at Tr = 5.

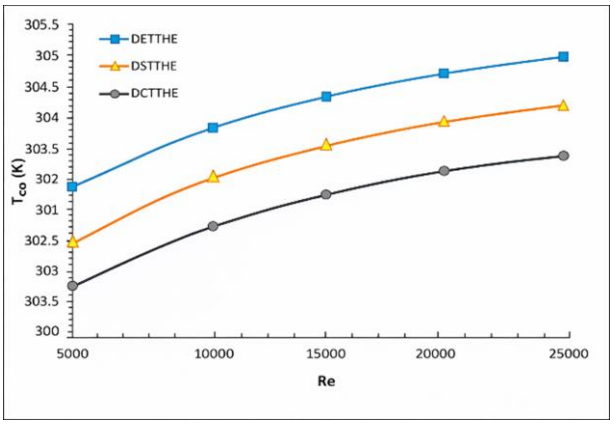


Fig. 3. Variation of the cold water outlet temperature with Reynolds number for DCTTHE, DSTTHE and DETTHE at Tr = 5.

contains internal twisting, its lower induced turbulence strength results in reduced thermal exchange, leading to lower outlet temperatures.

Figure 4 illustrates the temperature difference $T_h - T_c$ between hot and cold fluids for the three configurations at Tr = 5. The temperature difference decreases with the Reynolds number due to higher fluid velocity, with DCTTHE demonstrating the largest differential. This trend stems from the DETTHE's superior turbulence, which reduces T_{ho} by facilitating more efficient cold-fluid heat absorption.

The overall heat transfer coefficient (U) variation is depicted in Fig. 5. U rises with Reynolds number for all designs, driven

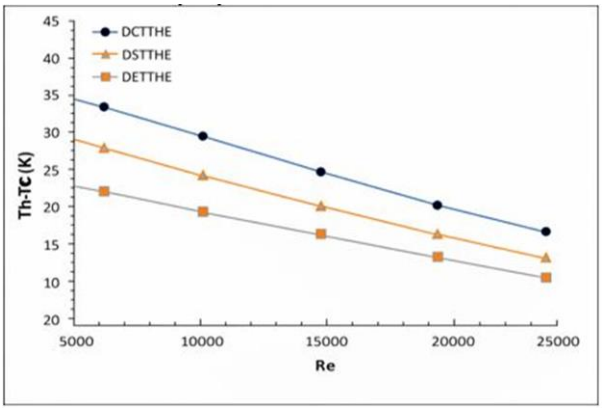


Fig. 4. Variation of the temperature difference between the hot and cold fluids with Reynolds number for DCTTHE, DETTHE and DSTTHE at Tr = 5.

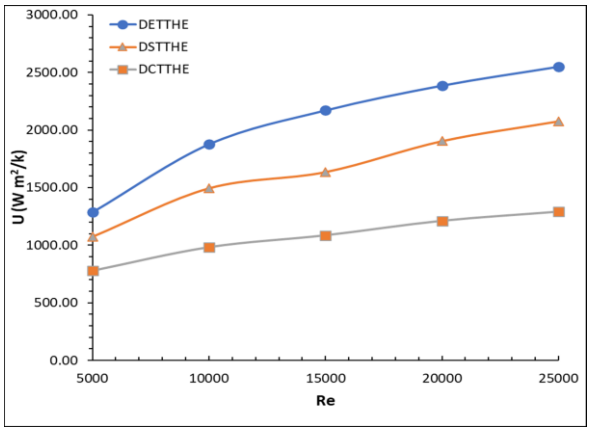


Fig. 5. Variation of the overall heat transfer coefficient with Reynold number for DCTTHE, DSTTHE and DETTHE at Tr = 5.

by greater thermal energy extraction from the hot fluid. DETTHE outperforms other designs due to vortices generated by its geometry, which amplify both heat transfer and pressure drop by disrupting the momentum boundary layer.

Figure 6 compares heat exchanger effectiveness (ϵ) across configurations. Effectiveness decreases at higher Re values due to a significant reduction in fluid residence time inside the tube.

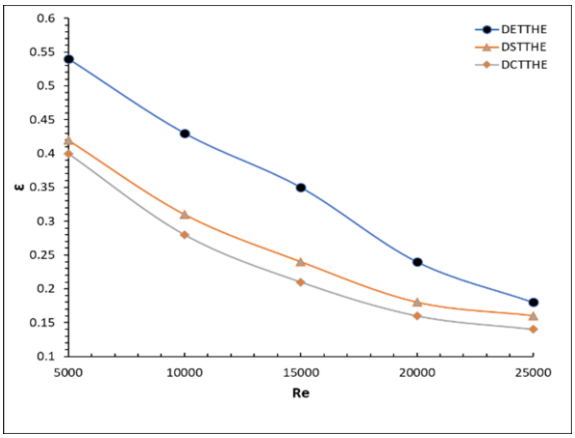


Fig. 6. Variation of the heat exchanger effectiveness with Reynolds number for DCTTHE, DETTHE and DSTTHE at Tr = 5.

At high flow velocities, the available time for heat exchange becomes insufficient to fully benefit from the increased heat transfer coefficient. Moreover, for the enhanced geometries (DETTH, DSTTHE and DCTTHE), the improvement in turbulence becomes less influential at high Reynolds numbers, while the associated pressure drop remains high, resulting in a relative decrease in effectiveness.

The Nusselt number trends are shown in Fig. 7. The Nu values increase with an increase in Reynolds number, as heightened turbulence thins the thermal boundary layer. For DETTHE, it surpasses those for other configurations due to its larger effective surface area and flow disruption.

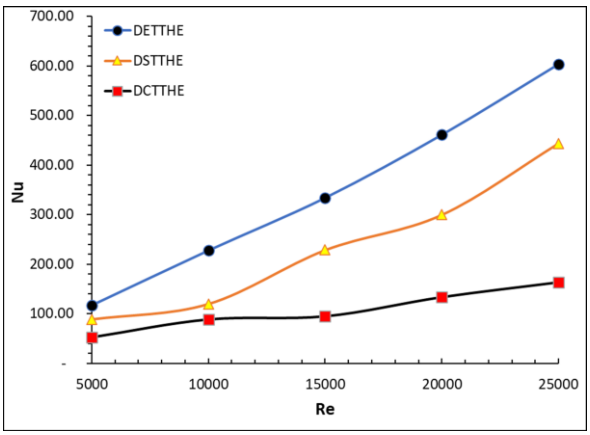


Fig. 7. Variation of the Nusselt number with Reynolds number for DCTTHE, DSTTHE and DETTHE at Tr = 5.

Pressure drop (ΔP_T) and average heat transfer rate (Q_{avg}) are analysed in Figs. 8 and 9, respectively. DETTHE incurs the highest ΔP_T due to intensified vortices, while also achieving the greatest Q_{avg} from enhanced fluid velocity and turbulence.

Finally, Fig. 10 evaluates the overall performance index (η). The value for DETTHE peaks at a lower Reynolds number (Re = 5000), exceeding the values for DCTTHE and DSTTHE by approximately 0.0025 and 0.0040, respectively. Performance declines across the Re range (Re = 5000–25 000) as pressure drop penalties outweigh thermal gains. Vortex generation, modulated by Tr = 5, critically influences this trade-off.

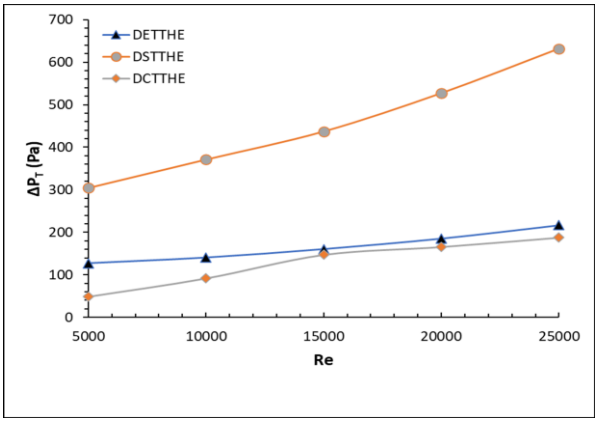


Fig. 8. Variation of the total pressure drop with Reynolds number for DCTTHE, DSTTHE and DETTHE at Tr = 5.

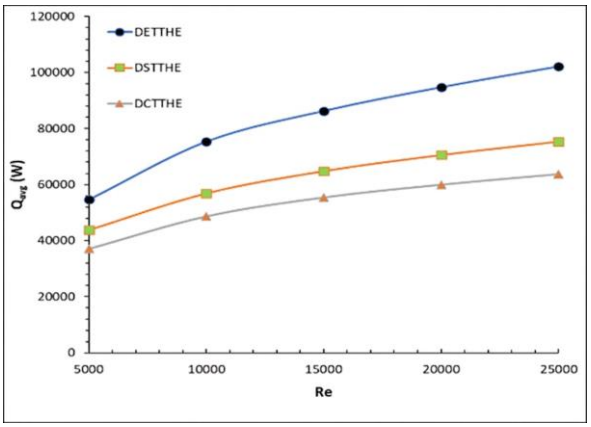


Fig. 9. Variation of average heat transfer rate with Reynolds number for DCTTHE, DSTTHE and DETTHE at Tr = 5.

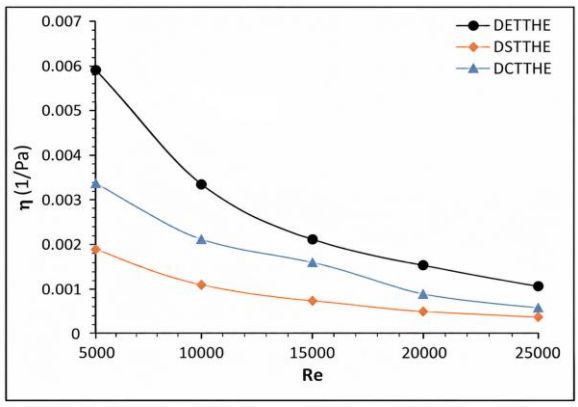
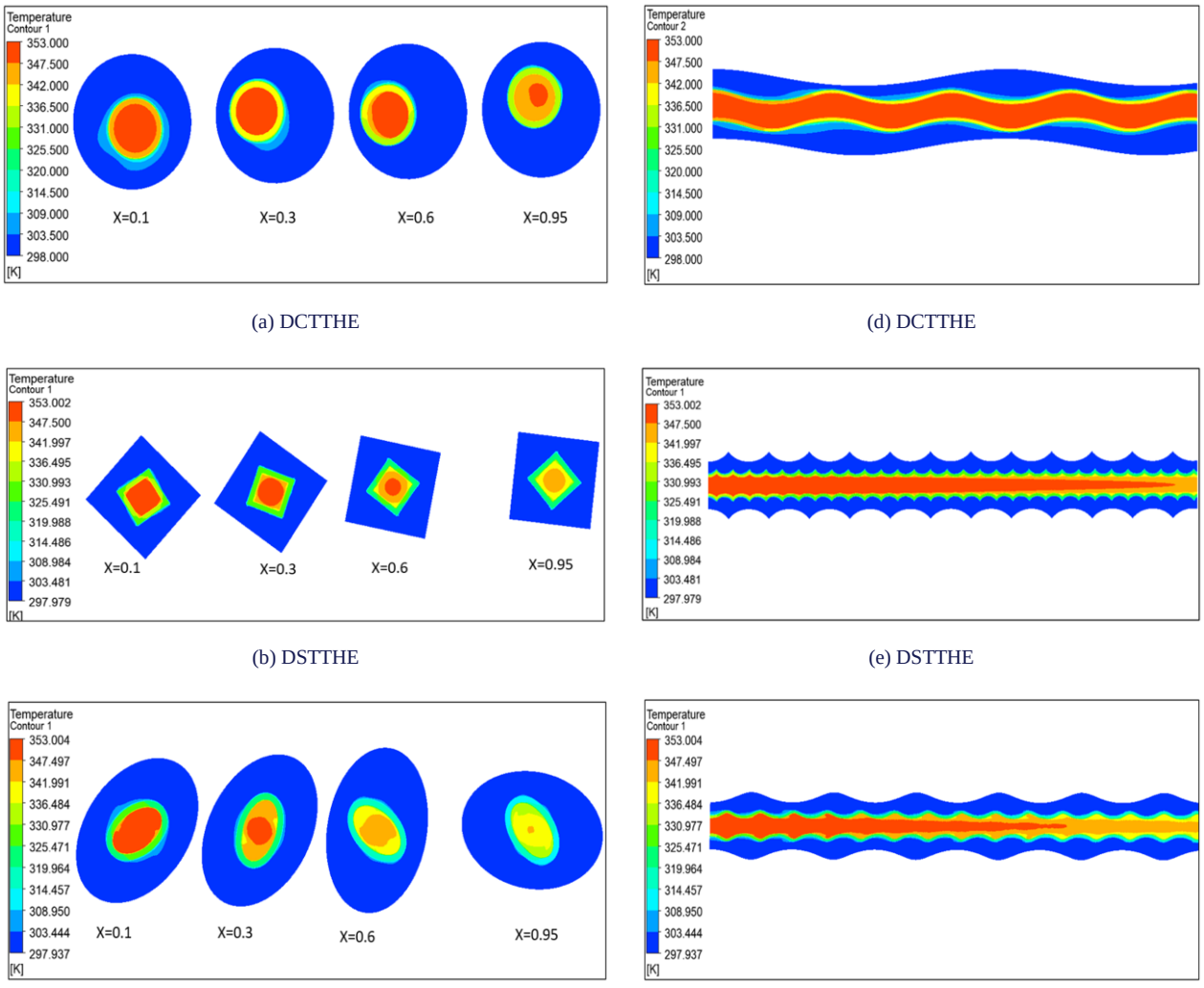


Fig. 10. Variation of the overall performance factor with Reynolds number for DCTTHE, DSTTHE and DETTHE at Tr = 5.

Figure 11 shows the temperature contours for various configurations of the double twisted tube heat exchanger – specifically DCTTHE, DSTTHE and DETTHE – at selected axial positions (0.1 m, 0.3 m, 0.6 m, and 0.95 m), under a Reynolds number of 25 000 and a twist ratio (Tr) of 5. At the inlet region, the temperature of the hot fluid is at its highest. As heat is transferred through the tube wall to the cold fluid, the temperature of the hot stream gradually decreases along the flow direction, reaching its



(a) DCTTHE

(d) DCTTHE

(b) DSTTHE

(e) DSTTHE

(c) DETTHE

(f) DETTHE

Fig. 11. Temperature distributions for DCTTHE, DSTTHE and DETTHE at Re = 25 000, Tr = 5.

lowest value near the outlet. The twisting in each configuration promotes thermal interaction between fluid layers, causing the bulk temperature at each cross-section to rise due to internal energy redistribution. This interlayer exchange enhances thermal equilibrium within the flow. The application of twisted geometries significantly improves temperature uniformity across circular, square and elliptical tube shapes. Notably, for all three designs, the highest temperature contours are observed near the outlet region (x = 0.95 m), indicating elevated thermal levels at the tube exit. At a twist ratio of 5, the inner wall's thermal boundary layer is disrupted by increased velocity and the development of secondary flows. The induced vortices intensify mixing within the fluid, leading to a progressive rise in temperature toward the outlet. The resulting temperature distribution around the inner tube surface exhibits a clear variation, emphasising the impact of twist-induced flow dynamics.

6. Conclusions

This study numerically evaluated the thermal and hydrodynamic performance of three twisted double tube heat exchanger configurations — circular (DCTTHE), square (DSTTHE) and elliptical (DETTHE) — under turbulent flow conditions with a fixed twist ratio of 5. The results demonstrated that the elliptical twisted tube (DETTHE) consistently outperformed the other geometries across all Reynolds numbers, exhibiting the highest Nusselt number, overall heat transfer coefficient and exchanger effectiveness. The enhanced performance is attributed to stronger secondary flows and turbulence generated by the elliptical twist, which improved fluid mixing and disrupted thermal boundary layers. DCTTHE exhibited the lowest thermal performance due to weaker turbulence generation, while DSTTHE showed intermediate results. Temperature distribution analysis confirmed more uniform heat transfer in DETTHE, particularly near the outlet. The study also found that performance gains were more pronounced at lower Reynolds numbers, with diminishing returns as flow velocity increased. While pressure drop increased with higher turbulence, DETTHE still achieved the best overall thermal-hydraulic performance. Temperature contour analysis further validated improved heat distribution and uniformity in the twisted configurations. These findings confirm that twisted elliptical designs significantly enhance heat transfer efficiency and are well-suited for industrial applications requiring compact and high-performance heat exchangers.

References

[1] Mushatet, K.S., Rishak, Q.A., & Fagr, M.H. (2020). Experimental and numerical investigation of swirling turbulent flow and heat transfer due to insertion of twisted tapes of new models in a heated tube. *Applied Thermal Engineering*, 171, 115070. doi: 10.1016/j.applthermaleng.2020.115070

[2] Razzaq, A.K.A., & Mushatet, K.S. (2023). A Review study for a twisted tube heat exchanger. *Journal of Nanofluid*s, 12(2), 299−317. doi: 10.1166/jon.2023.1926

[3] Salam, B., Biswas, S., Saha, S., & Bhuiya, M.M.K. (2013). Heat transfer enhancement in a tube using rectangular-cut twisted tape insert. *Procedia Engineering*, 56, 96−103. doi: 10.1016/j.proeng.2013.03.094

[4] Murali, G., Nagendra, B., & Jaya, J. (2020). CFD analysis on heat transfer and pressure drop characteristics of turbulent flow in a tube fitted with trapezoidal-cut twisted tape insert using Fe_3O_4 nano fluid. *Materials Today: Proceedings*, 21(1), 313−319. doi: 10.1016/j.matpr.2019.05.451

[5] Wu, C.C., Chen, C.C., Yang, Y.T., & Huang, K.H. (2018). Numerical simulation of turbulent flow forced convection in a twisted elliptical tube. *International Journal of Thermal Sciences*, 132, 199−208. doi: 10.1016/j.ijthermalsci.2018.05.028

[6] Cheng, J., Qian, Z., & Wang, Q. (2017). Analysis of heat transfer and flow resistance of twisted oval tube in low Reynolds number flow. *International Journal of Heat and Mass Transfer*, 109, 761−777. doi: 10.1016/j.ijheatmasstransfer.2017.02.061

[7] Luo, C., Song, K.W., & Tagawa, T. (2021). Heat transfer enhancement of a double pipe heat exchanger by co-twisting oval pipes with unequal twist pitches. *Case Studies in Thermal Engineering*, 28, 101411. doi: 10.1016/j.csite.2021.101411

[8] Alempour, S.M., Arani, A.A.A., & Najafizadeh, M.M. (2020). Numerical investigation of nanofluid flow characteristics and heat transfer inside a twisted tube with elliptic cross section. *Journal of Thermal Analysis and Calorimetry*, 140, 1237−1257. doi: 10.1007/s10973-020-09337-z

[9] Kim, H.R., Kim, S., Kim, M., Park, S.H., Min, J.K., & Ha, M.Y. (2016). Numerical study of fluid flow and convective heat transfer characteristics in a twisted elliptic tube. *Journal of Mechanical Science and Technology*, 30, 719−732. doi: 10.1007/s12206-016-0127-4

[10] Mushatet, K.S., & Youssif, F.K. (2018). Prediction the thermal and hydrodynamic performance of nano fluids flow in a tube coupled with double twisted tape. *ARPN Journal of Engineering and Applied Sciences*, 13(12), 4012−4021.

[11] Mushatet, K.S., & Youssif, F.K. (2018). Modeling whirling motion and heat transfer intensification in a heated tube with a twin twisted tape. *2018 International Conference on Advance of Sustainable Engineering and its Application ICASEA*, (pp. 215−220), 14–15 March, Wasit-Kut, Iraq. doi: 10.1109/ICASEA.2018.8370984

[12] Mashayekhi, R., Eisapour, A.H., Eisapour, M., Talebizadehsardari, P., Rahbari, A. (2022). Hydrothermal performance of twisted elliptical tube equipped with twisted tape insert. *International Journal of Thermal Sciences*, 172(A), 107233. doi: 10.1016/j.ijthermalsci.2021.107233

[13] Karimi, A., Al-Rashed, A.A., Afrand, M., Mahian, O., Wongwises, S., & Shahsavar, A. (2019). The effects of tape insert material on the flow and heat transfer in a nanofluid-based double tube heat exchanger: Two-phase mixture model. *International Journal of Mechanical Sciences*, 156, 397−409. doi: 10.1016/j.ijmecsci.2019.04.009

[14] Razzaq, A.K.A., & Mushatet, K.S. (2024). Influence of the twisting and nano fluids on performance of a triangular double tube heat exchanger. *Kerntechnik*, 89(3), 265−282. doi: 10.1515/kern-2023-0132

[15] Razzaq, A.K.A., & Mushatet, K.S. (2021). A numerical study for a double twisted tube heat exchanger. *International Journal of Heat & Technology*, 39(5), 1583−1589. doi: 10.18280/ijht.39052

[16] Razzaq, A.K.A., & Mushatet, K.S. (2024). Assessment the thermal performance of square twisted double tube heat exchanger with Al_2O_3 nanofluid. *Chemical Product and Process Modeling*, 19(4), 653−669. doi: 10.1515/cppm-2024-0047

[17] Razzaq, A.K.A., & Mushatet, K.S. (2021). Evaluation the performance of the double tube heat exchanger by using combined twisted tube and nano fluid. *International Journal of Mechanical Sciences*, 7(1), 6618−6628.